Keldysh Institute • Publication search

Keldysh Institute preprints • Preprint No. 87, 2016

ISSN 2071-2898 (Print)
ISSN 2071-2901 (Online)

Pichuzhkina A.V., Roldugin D.S.

Geomagnetic field models for satellite angular motion

Recommended form of bibliographic references: Pichuzhkina A.V., Roldugin D.S. Geomagnetic field models for satellite angular motion // Keldysh Institute Preprints. 2016. No. 87. 25 p. doi:10.20948/prepr-2016-87-e
URL: http://library.keldysh.ru/preprint.asp?id=2016-87&lg=e

О р д е н а Л е н и н а
ИНСТИТУТ ПРИКЛАДНОЙ МАТЕМАТИКИ
имени М.В. Келдыша
Р о с с и й с к о й а к а д е м и и н а у к

A.V. Pichuzhkina, D.S. Roldugin

Geomagnetic field models for satellite angular motion

Moscow — 2016

Пичужкина А.В., Ролдугин Д.С.

Использование моделей геомагнитного поля в задачах ориентации искусственных спутников Земли

Рассматриваются четыре модели геомагнитного поля: IGRF, наклонный и прямой диполи, осредненная модель. Для каждой модели приводятся выражения вектора индукции в разных системах координат, проводится сравнение моделей. Исследуются преимущества этих моделей при проведении аналитических исследований. Приводятся примеры моделирования углового движения спутника с магнитной системой ориентации в рамках различных моделей поля. Представлены соображения по использованию моделей в разных случаях.

Ключевые слова: магнитная система ориентации, геомагнитное поле

Alyona Pichuzhkina, Dmitry Roldugin

Geomagnetic field models for satellite angular motion

Four geomagnetic field models are discussed. These models are IGRF, inclined and right dipoles and averaged one. Geomagnetic induction vector is provided in different reference frames for these models. The vector motion is compared for different models. Models are used for analytical and numerical analysis. Preferred models for different cases are outlined.

Key words: magnetic attitude control system, geomagnetic field model

The work was supported by RFBR grant No. 15-31-20058.

Contents

Introduction

Magnetic attitude control systems, both active and passive, are widely used for CubeSats and other small satellites. The first satellite to be equipped with magnetic control was Transit 1B [1], launched April 13, 1960. The first satellite with active magnetic control was Tiros II [2], launched November 23, 1960. Magnetic field was first used for attitude determination aboard third Soviet satellite [3], launched May 15, 1958. Novel small satellites and especially CubeSats actively utilize the same principles. Here we outline some basic and modern works concerning magnetic attitude control.

Angular velocity damping is the main task for most magnetic control systems. The first concept was to use hysteresis rods [1,4–6]. This simple approach is still popular [7–11]. Spherical magnetic damper with viscous fluid [12] has no use now.

Active magnetic control systems are preferred aboard modern satellites. Magnetorquers have low cost, mass, power consumption and can be easily used even on CubeSats. “-Bdot” is the most common magnetic control algorithm. Published in [13] and first mentioned in [14], this algorithm was proposed by GSFC engineer Seymor Kant. Its investigation and in-flight performance analysis still attract interest [15–20].

Magnetic control can provide specific attitude regimes utilizing spin stabilization or auxiliary actuators. These are necessary to overcome underactuation issue: there is no control authority along the geomagnetic induction vector. Spin stabilization turns the satellite into a gyroscope. Spin axis attitude became fully controllable. Common schemes of one axis attitude control of spin stabilized satellites were proposed in [21,22]. Remarkable examples of analysis or implementation can be found in [2,13,23–29]. Spin stabilization allows promising optimal reorientation problems statements [30–32].

Auxiliary actuators, mainly gravity-gradient boom [33] or flywheel with constant speed [34–37] provide passive control authority necessary for stabilization in orbital reference frame. Fully magnetic control system may be used to provide any necessary attitude [38–43]. This relatively new and largely uncharted area is of special interest for small satellites.

Geomagnetic field model is necessary for attitude control and/or system design, on-board control computation and attitude determination process if magnetometer is used. Even passive magnetic system requires a model since attitude determination is still necessary for payload data interpretation. This paper focuses on models relevant for these applications. Four important models are introduced with exact expressions in different reference frames. Examples are discussed for analytical and numerical

analysis. Final recommendations are provided regarding different models implementation for specific purposes.

1. Geomagnetic field models

Reference frames

Four geomagnetic field models are considered: IGRF, inclined and direct dipoles and averaged (simplified dipole) model. Induction vector is expressed in a number of reference frames relevant for the satellite angular motion.

$O_aY_1Y_2Y_3$ is an inertial frame. O_a is Earth's center, O_aY_3 axis is directed along Earth's rotation axis, O_aY_1 lies in the equatorial plane and is directed to the ascending node of the circular orbit, O_aY_2 is directed so that the reference frame is right handed (the same holds for the following frames).

$O_aJ_1J_2J_3$ is J2000 inertial frame. O_aJ_3 axis is directed along Earth's rotation axis, O_aJ_1 is directed to the vernal equinox for the epoch 2000.0. Frames $O_aJ_1J_2J_3$ and $O_aY_1Y_2Y_3$ are tied by a rotation by the mean Greenwich time t_g about O_aJ_3 axis. Earth's axis precession is not taken into account.

$O_aZ_1Z_2Z_3$ is an inertial reference frame. It is got from $O_aY_1Y_2Y_3$ by turning by the angle Θ about O_aY_1 axis. This angle is defined with the averaged geomagnetic field model.

$O_aS_1S_2S_3$ inertial frame is bound the satellite's orbit. Axis O_aS_3 is normal to the equatorial plane. O_aS_1 is directed to the ascending node. Transition between frames $O_aY_1Y_2Y_3$ and $O_aS_1S_2S_3$ is represented by the angle i (orbit inclination) rotation about O_aY_1 axis. Transition between frames $O_aS_1S_2S_3$ and $O_aZ_1Z_2Z_3$ requires angle $\Theta - i$ rotation around O_aS_1. Inertial reference frames are depicted in Fig. 1.

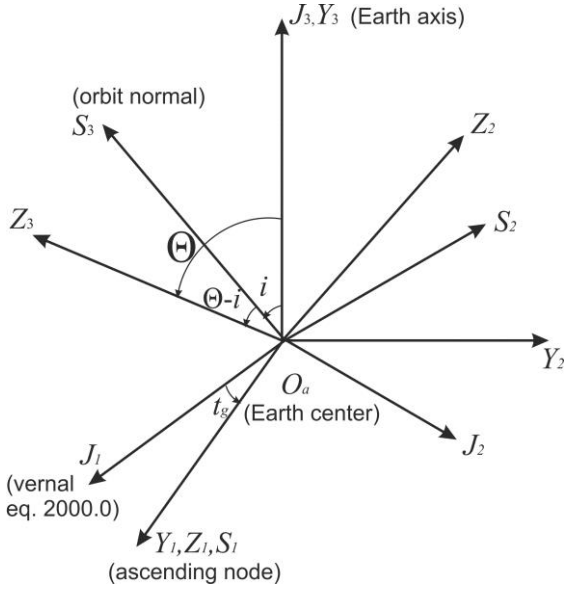

Fig. 1. Inertial reference frames

$OX_1X_2X_3$ is the orbital reference frame centered in the satellite's center of mass. OX_2 axis lies in the orbital plane. It is perpendicular to the radius-vector of the satellite. OX_2 is directed along the orbital angular velocity direction of a circular orbit. Axis OX_1 is directed along the radius vector. Axes sequence allows convenient reference frames transitions.

$Ox_1x_2x_3$ is the bound reference frame, it's axes coincide with the principal axes of inertia of the satellite.

$OL_1L_2L_3$ frame is bound to the satellite's angular momentum vector. OL_3 axis is directed along this vector. OL_2 axis lies in the plane of two first axes of inertial frame. Any inertial frame may be used depending on convenience and mission requirements of satellite motion representation (Fig. 7).

Vectors are supplemented with lower indices of corresponding reference frame where necessary. For example geomagnetic induction vector may be written as $\mathbf{B}_Y$ in $O_aY_1Y_2Y_3$ frame. Direction cosines matrices are

$$\mathbf{A}_{JY}=\begin{pmatrix}\cos t_g & \sin t_g & 0\\ -\sin t_g & \cos t_g & 0\\ 0 & 0 & 1\end{pmatrix},\ \mathbf{A}_{YZ}=\begin{pmatrix}1 & 0 & 0\\ 0 & \cos\Theta & \sin\Theta\\ 0 & -\sin\Theta & \cos\Theta\end{pmatrix},\ \mathbf{A}_{YS}=\begin{pmatrix}1 & 0 & 0\\ 0 & \cos i & \sin i\\ 0 & -\sin i & \cos i\end{pmatrix},$$

$$\mathbf{A}_{SX}=\begin{pmatrix}\cos u & \sin u & 0\\ -\sin u & \cos u & 0\\ 0 & 0 & 1\end{pmatrix},\qquad \mathbf{A}_{YX}=\mathbf{A}_{SX}\mathbf{A}_{YS}=\begin{pmatrix}\cos u & \sin u\cos i & \sin u\sin i\\ -\sin u & \cos u\cos i & \cos u\sin i\\ 0 & -\sin i & \cos i\end{pmatrix}$$

where u is the argument of latitude. Transition rule is $\mathbf{x}_j=\mathbf{A}_{ij}\mathbf{x}_i$.

International geomagnetic reference field / World magnetic model

IGRF (International geomagnetic reference field) and WMM (World magnetic model) are the most accurate models. Field decomposition is used in both models. It was proposed by C.F. Gauss in 1838. The decomposition is

$$V=-R\sum_{i=1}^{k}\left(\frac{R}{r}\right)^{i+1}\sum_{n=0}^{m}\left(g_n^m(t)\cos m\lambda_0+h_n^m(t)\sin m\lambda_0\right)P_n^m(\cos\vartheta_0),\ \mathbf{B}=\mu_0\nabla V$$

where λ_0 is the longitude of the point where the induction vector is calculated, $\vartheta=90^\circ-\theta_0$, θ_0 is the latitude of the point, r is the distance to the point from Earth's center, R is the average Earth radius. g_n^m and h_n^m are Schmitt coefficients given in a table [44], $\mu_0=4\pi\cdot10^{-7}$ kg·m·A^{-2}·s^{-2} is the magnetic vacuum permeability, P_n^m is a quasinormalised Legendre polynomial. Coefficients are derived empirically for both models. They are valid for five years. Coefficients are updated by International Union of Geodesy and Geophysics for IGRF model and by USA National Oceanic and

Atmospheric Administration for WMM. Models are designed for altitudes of no more than 600 km (relative to WGS84) though they may be used for higher orbits. These accurate models are often used onboard and in numerical simulation. IGRF is more widespread for satellite motion applications.

Inclined dipole

Inclined dipole model represents the major part of Gauss model. Three first terms are taken into account [45]. These terms describe the dipole tilted by a small angle to the opposite direction of Earth's rotation axis. Exact inclination angle varies as Earth's magnetic poles drift. This value is approximately 11.7° now. Dipole constitutes more than 90% of the field given by Gauss decomposition. Inclined dipole model takes into account two main sources of geomagnetic field variation: satellite motion along the orbit and Earth's rotation. Irregular effects (regions above highly magnetized areas) are not accounted for. Dipole geomagnetic induction vector is

$$\mathbf{B} = \frac{\mu_e}{r^5}\left(\mathbf{k}r^2 - 3(\mathbf{kr})\mathbf{r}\right)$$

where $\mathbf{k}$ is a unit dipole direction, $\mathbf{r}$ is the satellite's radius vector. Inclined dipole provides rather compact representation in $O_aY_1Y_2Y_3$ frame,

$$\mathbf{B}_Y = \frac{\mu_e}{r^3}\begin{pmatrix} \sin\lambda_2 \sin\delta_1 - 3\xi\cos u \\ -\cos\lambda_2 \sin\delta_1 - 3\xi\cos i\sin u \\ \cos\delta_1 - 3\xi\sin i\sin u \end{pmatrix}. \qquad (1.1)$$

Here $\mu_e = 7.812\cdot 10^6 km^3\cdot kg\cdot s^{-2}\cdot A^{-1}$ is Earth's magnetic constant, r is the radius-vector length. Angles λ_2, δ_1 provide dipole attitude with respect to $O_aY_1Y_2Y_3$ frame. Angle $\lambda_2 = \omega_E t + \lambda_{20}$ where ω_E is Earth's rotation rate represents dipole rotation with respect to $O_aY_1Y_2Y_3$,

$\xi = \cos u\sin\delta_1\sin\lambda_2 - \sin u\cos i\sin\delta_1\cos\lambda_2 + \sin u\cos\delta_1\sin i$, $\delta_1 \approx 168.3^\circ$. Transition matrices are used to represent induction vector in other reference frames. Bulky resulting expressions are omitted here. They are of no use for analytical approaches. Moreover numerical analysis often utilizes more compact and general relations using direction cosines matrices.

Direct dipole

Geomagnetic field model is further simplified by the direct dipole. Dipole unit vector is represented in $O_aY_1Y_2Y_3$ frame as $\mathbf{k} = (0,0,-1)$. Induction vector (1.1) is

$$\mathbf{B}_Y = \frac{\mu_e}{r^3}\begin{pmatrix} -1.5\sin i\sin 2u \\ -1.5\sin 2i\sin^2 u \\ 1-3\sin^2 i\sin^2 u \end{pmatrix}. \qquad (1.2)$$

Induction value changes along the orbit,

$$B_{0incl} = \frac{\mu_e}{r^3}\sqrt{1+3\sin^2 i \sin^2 u}\,. \qquad (1.3)$$

Reference frame $OX_1X_2X_3$ allows very compact field representation,

$$\mathbf{B}_X = \frac{\mu_e}{r^3}\begin{pmatrix} -2\sin u \sin i \\ \cos u \sin i \\ \cos i \end{pmatrix}. \qquad (1.4)$$

Frame $O_aS_1S_2S_3$ yields

$$\mathbf{B}_S = \frac{\mu_e}{r^3}\begin{pmatrix} -1.5\sin 2u \sin i \\ -3\sin^2 u \sin i + \sin i \\ \cos i \end{pmatrix}. \qquad (1.5)$$

Averaged model

Dipole geomagnetic induction vector unevenly rotates along the near-circular cone ($\mathbf{H}$-cone). The last simplification may be considered as averaging of this cone and induction vector motion. The cone becomes a circular one (Θ-cone) and induction vector moves uniformly [46]. It also has constant length. The cone is tangent to O_aY_3 and its axis lies in the $O_aY_2Y_3$ plane (Fig. 2).

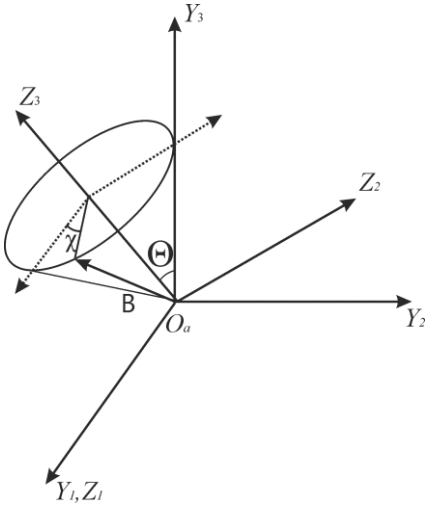

Fig. 2. Averaged geomagnetic model

Cone half angle is given by

$$\operatorname{tg}\Theta = \frac{3\sin 2i}{2\left(1-3\sin^2 i + \sqrt{1+3\sin^2 i}\right)}.$$

Vector rotates with double orbital angular velocity ω_0,

$$\chi = 2\omega_0 t + \chi_0 = 2u + \chi_0, \qquad (1.6)$$

geomagnetic induction vector in frame $O_aZ_1Z_2Z_3$ is

$$\mathbf{B}_Z = B_0 \begin{pmatrix} -\sin\Theta\sin\chi \\ \sin\Theta\cos\chi \\ \cos\Theta \end{pmatrix}. \qquad (1.7)$$

Phase χ_0 is found from the dipole and averaged models comparison. Induction vector is $\mathbf{B}_Z = B_0\left(0, \sin\Theta, \cos\Theta\right)^T$ if $\chi = 0$ from (1.7). It is directed along O_aY_3 axis (Fig. 2). Direct dipole model provides the same induction vector direction when $u = 0$ according to (1.2). Relation (1.6) then yields $\chi_0 = 0$.

Averaged model provides rather compact expressions:

$$OX_1X_2X_3 \quad \mathbf{B}_X = B_0 \begin{pmatrix} \sin i\sin u - 2\sin u\sin\Theta\left(\cos^2 u + \sin^2 u\cos\left(\Theta - i\right)\right) \\ \sin i\cos u + 2\cos u\sin\Theta\sin^2 u\left(1 - \cos\left(\Theta - i\right)\right) \\ -2\sin\Theta\sin^2 u\sin\left(\Theta - i\right) + \cos i \end{pmatrix} \qquad (1.8)$$

$$O_aZ_1Z_2Z_i \qquad \mathbf{B}_Z = B_0 \begin{pmatrix} -\sin\Theta\sin 2u \\ \sin\Theta\cos 2u \\ \cos\Theta \end{pmatrix} \qquad (1.9)$$

$$O_aY_1Y_2Y_3 \qquad \mathbf{B}_Y = B_0 \begin{pmatrix} -\sin\Theta\sin 2u \\ -\sin 2\Theta\sin^2 u \\ 1 - 2\sin^2\Theta\sin^2 u \end{pmatrix}$$

$$O_aS_1S_2S_3 \qquad \mathbf{B}_S = B_0 \begin{pmatrix} -\sin\Theta\sin 2u \\ -2\sin\Theta\sin^2 u\cos\left(\Theta - i\right) + \sin i \\ -2\sin\Theta\sin^2 u\sin\left(\Theta - i\right) + \cos i \end{pmatrix}$$

Averaged model is sometimes called a simplified dipole model. This model should be compared with the dipole model to prove its validity and find its parameters. Averaged induction vector length B_0 can be found from (1.3). Arithmetic mean between maximum and minimum dipole values is often used,

$$B_0 = \frac{1}{2}\left(B_{0incl}\left(0\right) + B_{0incl}\left(\frac{\pi}{2}\right)\right) = \frac{\mu_e}{2r^3}\left(1 + \sqrt{1 + 3\sin^2 i}\right). \qquad (1.10)$$

Integral mean is more accurate,

$$B_0 = \int_0^{\pi} B_{0incl}\left(u\right)du = \frac{\mu_e}{\pi r^3}\int_0^{\pi}\sqrt{1 + 3\sin^2 i\sin^2 u}\,du. \qquad (1.11)$$

Fig. 3 presents induction value for two approaches formalized by (1.10) and (1.11). These expressions provide close results. The difference is no more than 3% of the value. Simple expression (1.10) greatly facilitates analytical analysis. Numerical

simulation also benefits. Satellite motion along osculating orbit with changing inclination does not force numerical integration (1.11).

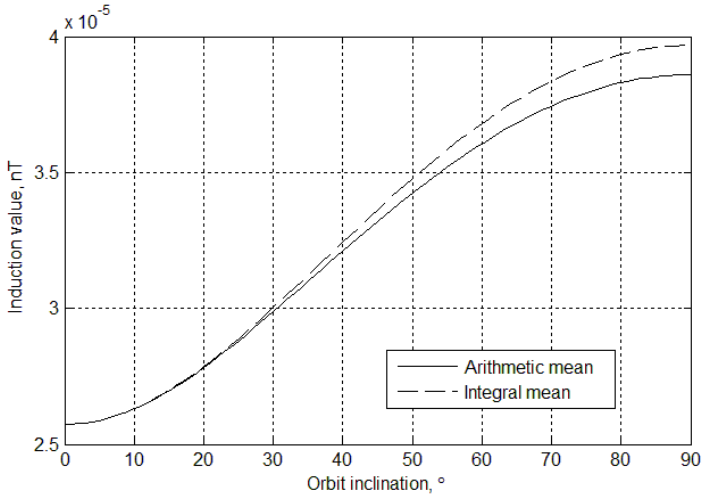

Fig. 3. Induction value at 350 km altitude

H- and Θ-cone comparison is ambiguous. Cones bases are different (Fig. 4). Θ-cone is a right one since geomagnetic induction vector has constant length. **H**-cone has tilted base according to changing induction value (1.3). Cones sides are close. Let δ be the angle between the dipole geomagnetic induction vector **B** and O_aZ_3 axis. Relation $\delta \geq \Theta$ is valid for every u ($\delta = \Theta$ if $u = 0$, $u = \pi/2$). This means that Θ-cone lies inside the **H**-cone. The cones have two diametrically opposite common lines. Difference $\delta - \Theta$ does not exceed 1°11'. Fig. 5 presents maximum deviation between two cones depending on the orbit inclination.

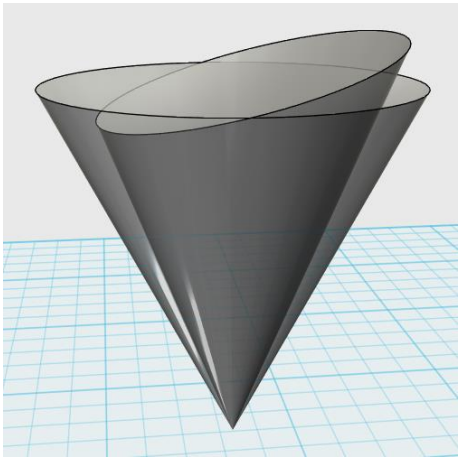

Fig. 4. **H**- and Θ-cones

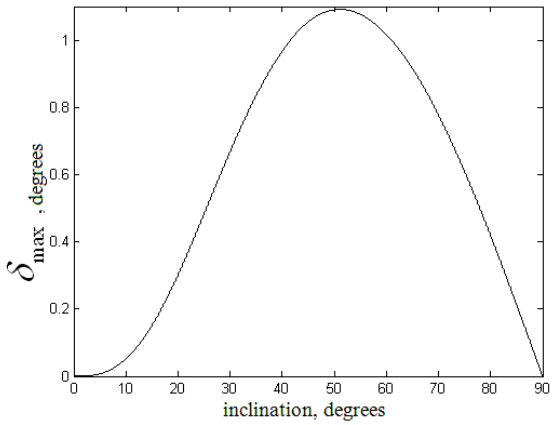

Fig. 5. Maximum deviation between two cones

Induction vectors should be compared for different values of orbit inclination and argument of latitude. Induction vectors coincide when $u = 0$, $u = \pi/2$ (they have

different lengths). Dipole induction vector gets ahead of the averaged one during the first quarter of the orbit. Second quarter provides opposite situation. Two vectors coincide after half of the orbital revolution. Let Δ be the maximum angular distance between these vectors. Expressions (1.4) and (1.8) are used to provide geomagnetic induction vector direction in different models but in the same reference frame. Induction vectors scalar product is

$$\cos\Delta = \frac{1+\sin^2 i \sin^2 u}{\sqrt{1+3\sin^2 i \sin^2 u}}. \qquad (1.12)$$

Its derivative is

$$\frac{d\cos\Delta}{di} = \frac{\sin^2 u \sin i \cos i \left(3\sin^2 i \sin^2 u - 1\right)}{\left(1+3\sin^2 i \sin^2 u\right)^{3/2}}.$$

It equals zero when $\sin i = 0$, $\cos i = 0$, $\sin^2 u = 1/(3\sin^2 i)$. Since $\sin^2 u \le 1$ extreme point implies that $1/\sqrt{3} \le |\sin i|$. Equality $\sin i = 1/\sqrt{3}$ corresponds to the inclination $i \approx 35^\circ$. Any greater inclination leads (1.12) to a stationary value.

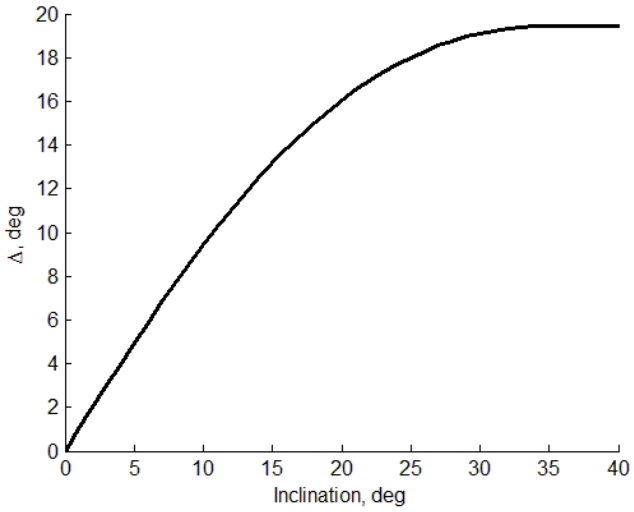

Fig. 6. Induction vectors maximum angular deviation Δ

Fig. 6 provides an insight into geomagnetic induction vectors difference in two models. They may deviate by up to 19 degrees from each other. Direct dipole and averaged geomagnetic models have close cones, but rather different induction vector motion. Averaged geomagnetic model cannot accommodate uneven induction vector rotation (as direct dipole does) and Earth rotation (as inclined dipole does). However this model provides generally adequate and compact field representation.

2. Analytical analysis examples

2.1. Transient motion

Transient motion represents the attitude acquiring phase, when angles and/or angular velocity are far from the necessary ones. It may refer to the angular velocity damping with high initial values for example. Osculating variables $L,\rho,\sigma,\varphi,\psi,\theta$ are used. Axisymmetrical satellite with inertia tensor $\mathbf{J}=diag\left(A,A,C\right)$ is considered. It moves along the circular orbit. Angular motion is described with equations [47]

$$\begin{aligned}
&\frac{dL}{dt}=M_{3L},\ \frac{d\rho}{dt}=\frac{1}{L}M_{1L},\ \frac{d\sigma}{dt}=\frac{1}{L\sin\rho}M_{2L},\\
&\frac{d\theta}{dt}=\frac{1}{L}\left(M_{2L}\cos\psi-M_{1L}\sin\psi\right),\\
&\frac{d\varphi}{dt}=L\cos\theta\left(\frac{1}{C}-\frac{1}{A}\right)+\frac{1}{L\sin\theta}\left(M_{1L}\cos\psi+M_{2L}\sin\psi\right),\\
&\frac{d\psi}{dt}=\frac{L}{A}-\frac{1}{L}M_{1L}\cos\psi\operatorname{ctg}\theta-\frac{1}{L}M_{2L}\left(\operatorname{ctg}\rho+\sin\psi\operatorname{ctg}\theta\right)
\end{aligned}\qquad (2.1)$$

where M_{1L},M_{2L},M_{3L} are the torque components, L is the angular momentum magnitude, angles ρ,σ represent angular momentum attitude with respect to any inertial frame. Fig. 7 utilizes $O_aZ_1Z_2Z_3$ as an example.

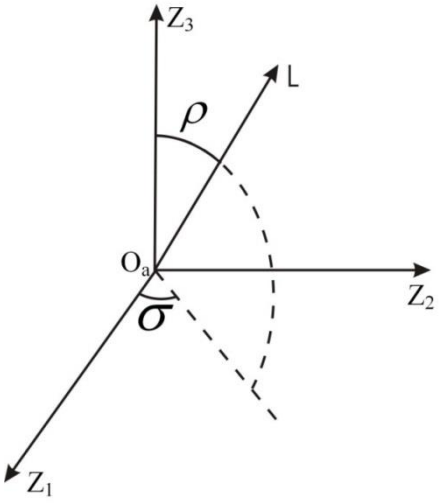

Fig. 7. Angular momentum attitude

Angular rate is characterized using only one variable L. Small control torque is assumed. This means that angular momentum change over one satellite or orbital revolution is small compared with the angular momentum itself. This is formalized with a small parameter ε. Equations of motion (2.1) have the form

$$\frac{d\mathbf{x}}{dt}=\varepsilon\mathbf{X}\left(\mathbf{x},\mathbf{y},t\right),\ \frac{d\mathbf{y}}{dt}=\mathbf{y}_0\left(\mathbf{x}\right)+\varepsilon\mathbf{Y}\left(\mathbf{x},\mathbf{y},t\right) \tag{2.2}$$

where $\mathbf{y}=\left(\varphi,\psi,u\right)^T$ are fast variables, $\mathbf{x}=\left(L,\rho,\sigma,\theta\right)^T$ are slow ones. Regular precession provides simple generating solution for equations (2.2). Averaging is independently performed over all fast variable and time. Accuracy of the averaged solution is of the order of ε for time interval of the order of $1/\varepsilon$.

Consider damping control torque [14]

$\mathbf{M}=k\left(\boldsymbol{\omega}\times\mathbf{B}\right)\times\mathbf{B}$,

$$\mathbf{M}_L=\begin{pmatrix}\omega_{3L}B_{1L}B_{3L}-\omega_{1L}B_{3L}^2-\omega_{1L}B_{2L}^2+\omega_{2L}B_{1L}B_{2L}\\ \omega_{1L}B_{1L}B_{2L}-\omega_{2L}B_{1L}^2-\omega_{2L}B_{3L}^2+\omega_{3L}B_{2L}B_{3L}\\ \omega_{2L}B_{2L}B_{3L}-\omega_{3L}B_{2L}^2-\omega_{3L}B_{1L}^2+\omega_{1L}B_{1L}B_{3L}\end{pmatrix}. \tag{2.3}$$

Following results are based on [19]. Averaging involves expressions $\left\langle M_{iL}\right\rangle_{u,\varphi,\psi}$, $\left\langle M_{iL}\cos\psi\right\rangle_{u,\varphi,\psi}$ and $\left\langle M_{iL}\sin\psi\right\rangle_{u,\varphi,\psi}$. This necessitates calculation of

$$B_{ij}=\frac{1}{2\pi}\int_0^{2\pi}B_iB_j du,\ \left(i,j=1,2,3\right) \tag{2.4}$$

where B_i are dimensionless geomagnetic induction vector components.

Averaged equations simplicity is largely governed by (2.4). We use the most convenient inertial reference frame for each model. The goal is to find the simplest averaged equations of motion. Angular momentum magnitude may be compared in different reference frames since it is a scalar variable.

Averaged geomagnetic field model has the most compact form (1.9) in the reference frame $O_aZ_1Z_2Z_3$. Expressions (2.4) are

$$B_{11}=B_{22}=p=\frac{1}{2}\sin^2\Theta,\ B_{33}=q=\cos^2\Theta,\ B_{12}=B_{23}=B_{13}=0$$

and averaged equations of motion for slow variables l,ρ,σ,θ are

$$\begin{aligned}
&\frac{dl}{du}=-\varepsilon l\left[2p+\left(1-3p\right)\sin^2\rho\right]\left(\cos^2\theta+\frac{C}{A}\sin^2\theta\right),\\
&\frac{d\rho}{du}=\varepsilon\left(3p-1\right)\sin\rho\cos\rho\left(\cos^2\theta+\frac{C}{A}\sin^2\theta\right),\\
&\frac{d\sigma}{du}=0,\\
&\frac{d\theta}{du}=\frac{1}{2}\varepsilon\left(1-\frac{C}{A}\right)\left[2\left(1-p\right)+\left(3p-1\right)\sin^2\rho\right]\sin\theta\cos\theta.
\end{aligned} \tag{2.5}$$

Equations (2.5) allow the full set of the first integrals [19]. These integrals are found in the exact form. Equations (2.5) are therefore directly solved in quadratures.

Dipole model has the most compact form (1.5) in the inertial frame $O_aS_1S_2S_3$. Angles ρ,σ represent angular momentum attitude with respect to this frame. Expressions (2.4) provide

$$B_{11}=a=\frac{9}{8}\sin^2 i,\ B_{22}=\frac{11}{9}a=\frac{11}{8}\sin^2 i,\ B_{12}=B_{13}=0,$$

$$B_{23}=d=-\frac{1}{2}\sin i\cos i,\ B_{33}=c=\cos^2 i.$$

Averaging leads to

$$\frac{dl}{du}=-\varepsilon l\left[\frac{20}{9}a+\sin^2\rho\left(c-a\cos^2\sigma-\frac{11}{9}a\sin^2\sigma\right)+2d\cos^2\rho\sin\sigma\cos\sigma\right]\times$$

$$\times\left(\cos^2\theta+\frac{C}{A}\sin^2\theta\right),$$

$$\frac{d\rho}{du}=\varepsilon\left[\left(\frac{11}{9}a\sin^2\sigma+a\cos^2\sigma-c\right)\sin\rho\cos\rho-d\sin\sigma\cos 2\rho\right]\left(\cos^2\theta+\frac{C}{A}\sin^2\theta\right),$$

$$\frac{d\sigma}{du}=\varepsilon\left[\frac{2}{9}a\sin\sigma\cos\sigma+d\cos\sigma\operatorname{ctg}\rho\right]\left(\cos^2\theta+\frac{C}{A}\sin^2\theta\right),$$

$$\frac{d\theta}{du}=\varepsilon\lambda\left[\frac{20}{9}a+c\left(1+\cos^2\rho\right)+a\sin^2\rho\left(\cos^2\sigma+\frac{11}{9}\sin^2\sigma\right)+2d\sin\rho\cos\rho\sin\sigma\right]\times$$

$$\times\sin\theta\cos\theta.$$

Small parameter ε changes but retains its meaning – small change in angular momentum. Averaged equations include one more term due to the "non-diagonal" element B_{23}. Only some first integrals are available. Expressions for derivatives of ρ $/\sigma$ and l/ρ may be grouped to find two integrals in quadratures.

Inclined dipole model necessitates additional averaging over Earth's rotation. Expressions B_{ij} can be found using geomagnetic induction vector expressed in $O_aY_1Y_2Y_3$ frame (1.1). This leads to

$$B_{11}=\frac{11}{16}\sin^2\delta_1+\frac{9}{8}\left(\cos^2\delta_1\sin^2 i+\frac{1}{2}\cos^2 i\sin^2\delta_1\right),$$

$$B_{22}=\frac{1}{2}\sin^2\delta_1-\frac{15}{16}\cos^2 i\sin^2\delta_1+\frac{27}{8}\cos^2 i\left(\cos^2\delta_1\sin^2 i+\frac{1}{2}\cos^2 i\sin^2\delta_1\right),$$

$$B_{33} = \cos^2\delta_1 + \frac{9}{16}\sin^2 i\sin^2\delta_1 - 3\sin^2 i\cos^2\delta_1 + \frac{27}{8}\sin^2 i\left(\cos^2\delta_1\sin^2 i + \frac{1}{2}\cos^2 i\sin^2\delta_1\right),$$

$$B_{12} = 0,\ B_{13} = 0,$$

$$B_{23} = -\frac{3}{2}\sin i\cos i\left(\cos^2\delta_1 + \frac{1}{8}\sin^2\delta_1\right) + \frac{27}{8}\sin i\cos i\left(\sin^2 i\cos^2\delta_1 + \frac{1}{2}\cos^2 i\sin^2\delta_1\right).$$

These expressions are clearly overburdened. Transient motion analysis allows the deepest results with the averaged geomagnetic field model.

2.2. Motion in the vicinity of necessary attitude

Attitude accuracy in the vicinity of necessary position is represented with the Euler equations. Satellite motion is described with absolute angular velocity components $\omega_1, \omega_2, \omega_3$ and angles α, β, γ. These angles represent frame $Ox_1x_2x_3$ attitude with respect to $OX_1X_2X_3$. Direction cosines matrix **D** is

$$\mathbf{D} = \begin{pmatrix} \cos\alpha\cos\beta & \sin\beta & -\sin\alpha\cos\beta \\ -\cos\alpha\sin\beta\cos\gamma + \sin\alpha\sin\gamma & \cos\beta\cos\gamma & \sin\alpha\sin\beta\cos\gamma + \cos\alpha\sin\gamma \\ \sin\alpha\cos\gamma + \cos\alpha\sin\beta\sin\gamma & -\cos\beta\sin\gamma & -\sin\alpha\sin\beta\sin\gamma + \cos\alpha\cos\gamma \end{pmatrix}.$$

Dynamical equations of the satellite with inertia tensor $\mathbf{J} = \mathrm{diag}(A, B, C)$ are

$$A\frac{d\omega_1}{dt} + (C - B)\omega_2\omega_3 = M_{1x},$$

$$B\frac{d\omega_2}{dt} + (A - C)\omega_1\omega_3 = M_{2x},$$

$$C\frac{d\omega_3}{dt} + (B - A)\omega_1\omega_2 = M_{3x},$$

kinematic equations are

$$\frac{d\alpha}{dt} = \frac{1}{\cos\beta}(\omega_2\cos\gamma - \omega_3\sin\gamma - \omega_0\sin\alpha\sin\beta),$$

$$\frac{d\beta}{dt} = \omega_2\sin\gamma + \omega_3\cos\gamma - \omega_0\cos\alpha, \qquad (2.6)$$

$$\frac{d\gamma}{dt} = \omega_1 - \mathrm{tg}\,\beta(\omega_2\cos\gamma - \omega_3\sin\gamma) + \omega_0\frac{\sin\alpha}{\cos\beta}.$$

Planar motion

Consider the satellite that moves on a polar orbit in a gravitational field. This motion satisfies

$\alpha = \gamma = 0$, $\omega_1 = \omega_2 = 0$.

Planar motion also exists for some control strategies. Suppose that magnetic control dipole moment is $\mathbf{m} = (m, 0, 0)^T$. Constant magnet along a principal axis is a good example. Control torque for this case is

$\mathbf{M}_{ctrl} = \mathbf{m} \times \mathbf{B}_x = B_0 (0, -mB_{x3}, mB_{x2})^T$.

Averaged and dipole models provide $B_{x3} = 0$. Inclined dipole model does not allow planar motion since $B_{x3} = \cos\lambda_2 \sin\delta_1 \neq 0$. The dipole does not lie in the orbital plane. This model cannot be used in the following analytical analysis. Planar motion is described by the equation

$$C\ddot{\beta} = 3\omega_0^2 (A-B)\sin\beta\cos\beta + mB_0 (\cos(\beta - u) + \kappa \sin u \sin\beta) \qquad (2.7)$$

where $\kappa = 0$ for the averaged model and $\kappa = 1$ for the dipole model. Constant magnet is used to assure satellite motion with the geomagnetic induction vector. Nominal attitude regime corresponds to the magnet coinciding with the induction vector. We concentrate on this regime possibility and analysis. Consider motion in the vicinity of necessary ideal attitude,

$\beta = \beta_0 + \Delta\beta$

where β_0 is the geomagnetic induction vector direction, $\Delta\beta$ determines attitude accuracy. Averaged model yields $\beta_0 = \arcsin(\cos u)$. Linearized equation (2.7) is

$$\Delta\ddot{\beta} + \Delta\beta (\lambda^2 + \varepsilon\cos 2u) = -\varepsilon/2 \cdot \sin 2u \qquad (2.8)$$

where $\varepsilon = \dfrac{3(A-B)}{C}$, $\lambda^2 = \dfrac{mB_0}{C\omega_0^2}$. Equation (2.8) is quasiharmonic. Autonomous oscillations are described as

$$\Delta\ddot{\beta} + \Delta\beta\lambda^2 (1 + \varepsilon/\lambda^2 \cos 2u) = 0. \qquad (2.9)$$

This is a well-known Mathieu equation. Parameters λ and ε govern system stability. System (2.9) is stable if only control magnetic torque acts on the satellite ($\varepsilon = 0$). System may become unstable as parameter ε (gravitational torque value) rises in comparison with λ (control torque value). We aim to find unstable areas in ε-λ space as described in [48]. Non-homogeneous part in (2.8) governs attitude accuracy. This quantitative attitude performance measure is not taken into account.

Characteristic equation for (2.9) is

$$\rho^2 - 2A(\lambda, \varepsilon/\lambda^2)\rho + 1 = 0 \qquad (2.10)$$

and its roots are

$\rho(\lambda, \varepsilon/\lambda^2) = A \pm \sqrt{A^2 - 1}$.

Stability areas of equation (2.9) require $A^2<1$ (two imaginary roots with unit modulus). Unstable areas are observed if $A^2>1$ (two real roots). Stable and unstable areas are divided by λ values that satisfy either

$$A\left(\lambda,\varepsilon/\lambda^2\right)=+1 \tag{2.11}$$

or

$$A\left(\lambda,\varepsilon/\lambda^2\right)=-1. \tag{2.12}$$

Consider no gravitational torque influence. Characteristic exponents of (2.10) are $\pm\lambda i$ if $\varepsilon/\lambda^2=0$. The roots are

$$\rho_1(\lambda,0)=e^{\pi\lambda i},\quad \rho_1(\lambda,0)=e^{-\pi\lambda i}$$

and therefore

$$A(\lambda,0)=1/2\left(\rho_1+\rho_2\right)=\cos\pi\lambda.$$

Parameter $A\left(\lambda,\varepsilon/\lambda^2\right)$ is an analytical function of λ and ε/λ^2 [48]. We represent it as

$$A\left(\lambda,\varepsilon/\lambda^2\right)=\cos\pi\lambda+\varepsilon/\lambda^2\cdot F\left(\lambda,\varepsilon/\lambda^2\right) \tag{2.13}$$

where $F\left(\lambda,\varepsilon/\lambda^2\right)$ is an analytical function.

Conditions (2.11) and (2.12) are satisfied if $\varepsilon/\lambda^2=0$ and $\lambda=n$ where n is a positive integer. Small $\varepsilon/\lambda^2\neq 0$ leads to (2.11) solutions with respect to λ in the vicinity of every even number. Equation (2.12) possesses solutions in the vicinity of odd numbers. Solutions are real and may be represented as convergent series

$$\lambda^2=n^2+\alpha_1\varepsilon/\lambda^2+\alpha_1\left(\varepsilon/\lambda^2\right)^2+... \tag{2.14}$$

Equation (2.9) possesses a π-periodical solution if (2.11) is satisfied. Relation (2.12) forces the solution to satisfy $f\left(t+\pi\right)=-f\left(t\right)$ so it is 2π-periodical. Equation (2.9) solution is represented by a series

$$\Delta\beta=\Delta\beta_0(u)+\varepsilon/\lambda^2\cdot\Delta\beta_1(u)+\left(\varepsilon/\lambda^2\right)^2\cdot\Delta\beta_2(u)+... \tag{2.15}$$

Here $\Delta\beta_0$ is a periodical solution in case $\varepsilon/\lambda^2=0$. Consider the first unstable area that corresponds to $n=1$. Expressions (2.14) and (2.15) are substituted to (2.9) leading to $\alpha_1=\pm1/2$, $\alpha_2=7/32$. The first unstable area is

$$1-\frac{\varepsilon}{2\lambda^2}+\frac{7}{32}\left(\frac{\varepsilon}{\lambda^2}\right)^2+...\le\lambda^2\le1+\frac{\varepsilon}{2\lambda^2}+\frac{7}{32}\left(\frac{\varepsilon}{\lambda^2}\right)^2+...$$

Dipole model ($\kappa = 1$) complicates equation (2.7). It has compact form near ascending and descending nodes of the orbit. In this case $\beta_0 = \arcsin\left(\cos u\right)\Big/\sqrt{1+3\sin^2 u}$ and

$$\Delta\ddot{\beta} + \Delta\beta\left(\frac{3\lambda^2}{2} + \frac{2\varepsilon - \lambda^2}{2}\cos 2u\right) = \frac{\lambda^2 - \varepsilon}{2}\sin 2u$$

where $\lambda^2 = \dfrac{m\mu_e}{r^3 C\omega_0^2}$. The first unstable are is

$$1 - \frac{2\varepsilon - \lambda^2}{6\lambda^2} + \frac{7}{32}\left(\frac{2\varepsilon - \lambda^2}{3\lambda^2}\right)^2 + \ldots \le \lambda^2 \le 1 + \frac{2\varepsilon - \lambda^2}{6\lambda^2} + \frac{7}{32}\left(\frac{2\varepsilon - \lambda^2}{3\lambda^2}\right)^2 + \ldots$$

Expressions for the first unstable area may be compared for two geomagnetic field models. This area shrinks as values ε/λ^2 (averaged model) or $\left(2\varepsilon - \lambda^2\right)\Big/3\lambda^2 = 2\varepsilon/3\lambda^2 - 1/3$ (direct dipole model) lower. Parameter $\varepsilon/\lambda^2 = 3\left|A - B\right|\omega_0^2/mB_0$ depends heavily on the gravitational torque value. Axisymmetrical satellite provides good extreme case. Gravitational torque is zeroed and unstable area vanishes completely. Satellite motion is governed by the control torque only. Permanent magnet coincides with the geomagnetic induction vector and this position is stable.

Direct dipole model involves more complicated expression $\left(2\varepsilon - \lambda^2\right)\Big/3\lambda^2 = 2\left|A - B\right|\omega_0^2/mB_0 - 1/3$. It is close to zero if $\left|A - B\right|\omega_0^2/mB_0 \approx 1/6$. Unstable area vanishes if $\left|A - B\right|\omega_0^2/mB_0 \le 1/6$. Satellite and orbit parameters that provide guaranteed stability are broadened. Satellite does not need to be axisymmetrical. Its inertia moments should satisfy a relation that ensures small enough gravitational torque.

Averaged geomagnetic field model allows quantitatively correct result. Direct dipole model provides more accurate and general result. This comes at the cost of one excessive restriction.

Spatial motion

Satellite equipped with a flywheel is considered. This allows the satellite to acquire inherent constant angular momentum. The flywheel is designed for this angular momentum to prevail over the satellite's one (wheel has high angular rate and/or mass). The satellite-wheel system behaves like a gyro in the inertial space. Dynamical equations of motion are

$$\mathbf{J}\dot{\boldsymbol{\omega}} + \boldsymbol{\omega}\times\mathbf{J}\boldsymbol{\omega} + \boldsymbol{\omega}\times\mathbf{h} = \mathbf{M}_{gr} + \mathbf{M}_{ctrl} \qquad (2.16)$$

where $\mathbf{h}=(0,\,0,\,1)^T$ for the flywheel directed along the third principal axis of the satellite. Poincare method [48] is used for equations (2.16)-(2.6) analysis. These equations have general form

$$\frac{d\mathbf{x}}{du}=\mathbf{f}(\mathbf{x})+\varepsilon\mathbf{g}(\mathbf{x})$$

where $\mathbf{x}=(\omega_1,\omega_2,\omega_3,\alpha,\beta,\gamma)^T$, $\mathbf{f}(\mathbf{x})$ are gyroscopic and gravitational torques, $\varepsilon\mathbf{g}$ is a control torque, ε is a small parameter. Specific ε expression depends on the control algorithm used. Solution is decomposed into a series $\mathbf{x}=\mathbf{x}_0+\varepsilon\mathbf{x}_1$ and equations are

$$\frac{d\mathbf{x}_0}{du}+\varepsilon\frac{d\mathbf{x}_1}{du}=\mathbf{f}(\mathbf{x}_0)+\varepsilon\left(\mathbf{F}(\mathbf{x}_0)\mathbf{x}_1+\mathbf{g}(\mathbf{x}_0)\right)+O(\varepsilon^2) \qquad (2.17)$$

where $F_{ij}=\partial f_i/\partial x_j$. Solution $\mathbf{x}_0=(0,\,0,\,1,\,0,\,0,\,0)^T$ is used as a generating one. It represents precise conjunction of the orbital and bound reference frames. This equilibrium position is stable if proper inertia moments are chosen. Damping magnetic control is implemented to provide asymptotic stability for this equilibrium position. The control is [14]

$$\mathbf{M}_{ctrl}=-k\frac{d\mathbf{B}_x}{dt}\times\mathbf{B}_x.$$

Solution (2.17) should be substituted to the equations of motion (2.16)-(2.6). First order approximation $\mathbf{x}_1$ satisfies equations

$$\frac{d\omega_1}{du}=-\theta_A\omega_2+\frac{k}{A\omega_0}\left(\frac{\mu_e}{r^3}\right)^2\sin u\sin i\cos i,$$

$$\frac{d\omega_2}{du}=\theta_B\omega_1-3\lambda_B\alpha-2\frac{k}{B\omega_0}\left(\frac{\mu_e}{r^3}\right)^2\cos u\sin i\cos i,$$

$$\frac{d\omega_3}{du}=3\lambda_C\beta+2\frac{k}{C\omega_0}\left(\frac{\mu_e}{r^3}\right)^2\sin^2 i,$$

$$\frac{d\alpha}{du}=\omega_2-\gamma,\quad \frac{d\beta}{du}=\omega_3,\quad \frac{d\gamma}{du}=\omega_1+\alpha.$$

In-plane motion is detached. It is described by the equation

$$\ddot{\beta}-3\lambda_C\beta=2\frac{k}{C\omega_0}\left(\frac{\mu_e}{r^3}\right)^2\sin^2 i\,.$$

Inertia moments of the satellite ensure $\lambda_C < 0$. Homogeneous part solution is oscillation near equilibrium position. Attitude accuracy is determined by the partial solution

$$\beta = -\frac{2k}{3\lambda_C C\omega_0}\left(\frac{\mu_e}{r^3}\right)^2 \sin^2 i. \qquad (2.18)$$

Averaged geomagnetic field model leads to overburdened equations of motion. They have quite compact form only for a polar orbit. Planar motion for this case is governed by the equation

$$\ddot{\beta} - 3\lambda_C \beta = \frac{k}{C\omega_0} B_0^2,$$

Partial solution is

$$\beta = -\frac{3k}{4\lambda_C C\omega_0}\left(\frac{\mu_e}{r^3}\right)^2.$$

Solution (2.18) applied for a polar orbit is

$$\beta = -\frac{2k}{3\lambda_C C\omega_0}\left(\frac{\mu_e}{r^3}\right)^2.$$

Both solutions differ slightly. Direct dipole model is intuitively more accurate and therefore preferable. Moreover it provides more general result valid for any orbit inclination. Averaged model allows compact result only for a polar orbit. The accuracy estimate is more pessimistic. This estimate may be preferable for the attitude system design process with the worst possible situation in mind.

3. Numerical simulation

Analytical analysis was based on a number of representative examples. These are now assessed numerically. Numerical simulation is an inherent part of the attitude system design. Attitude hardware parameters and algorithms are chosen based on the results of the simulation and general results provided by the analytical study.

Angular velocity damping is the first example. Damping effectiveness is characterized by the time necessary to lower angular velocity to a certain amount. This time differs depending on the geomagnetic model used.

Simulation parameters are:

- Inertia tensor $\mathbf{J} = \mathrm{diag}(5750, 2450, 4000)$ *kg·m²*
- Orbit altitude 1000 *km*
- Inclination 82.5°

- Damping control gain $k = 5 \cdot 10^{11}$ $N \cdot m \cdot s / T^2$ (magnetorquers are capped at 250 $A \cdot m^2$ maximum dipole moment)
- Initial attitude angles are 60, 130, 230 degrees (rotation sequence 1-3-2)
- Initial angular rate (0.001, 0.002, 0.003) s^{-1}.

Gravitational and control torques are taken into account. Satellite motion is described in the orbital reference frame. Fig. 8 provides numerical simulation results.

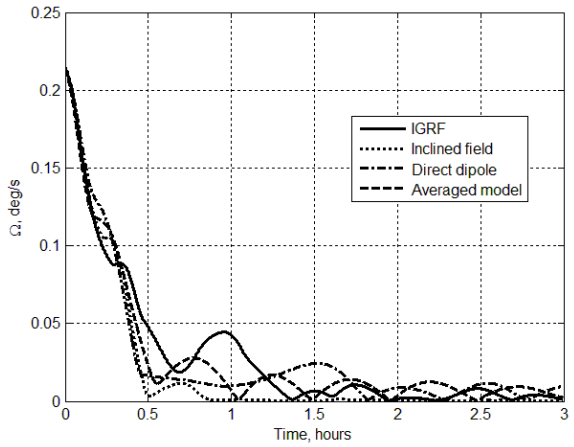

Fig. 8. Angular velocity damping

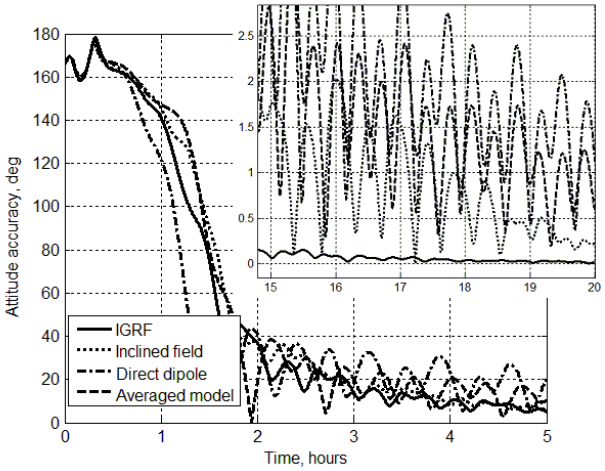

Fig. 9. Flywheel reorientation

Angular velocity damping times differ slightly. Main damping process takes about 0.5 hour for each model. Two dipole models provide especially close results. IGRF model provides the worst damping efficiency. Simplified geomagnetic field models may be used for transient motion analysis. Numerical analysis complexity greatly benefits from simple models. Simulation with IGRF model took 147.7 seconds (128.5 seconds for model calculation). Inclined field required only 33.8 seconds, direct dipole – 15 seconds, averaged model – 14.8 seconds.

Fig. 9 provides another transient motion example. Satellite is equipped with a flywheel. Angle between the flywheel axis and orbital normal is depicted in Fig. 9. Flywheel angular momentum is 10 $N \cdot m \cdot s$, damping control parameter is ten times less, initial attitude angles are 60, 100 and 230 degrees. Transient motion result is close for different geomagnetic field models.

Fig. 8 and 9 provide preliminary insight into attitude accuracy results with different models. Accuracy is affected by the model. Following simulation examples are obtained with two additional assumptions. Disturbing torque is taken into account (constant torque of the order of $1 \cdot 10^{-4}$ $N \cdot m$ in bound frame and Gaussian disturbance of the order of $4 \cdot 10^{-4}$ $N \cdot m$). Attitude determination error is introduced (1° bias and 2° normal distribution for angles, 0.01 *deg/s* and 0.001 *deg/s* for angular velocity). Fig. 10 provides simulation result. Maximum angle between bound and orbital frames

axes pairs is chosen as an attitude accuracy measure. Initial attitude angles are 6, 3, 2 degrees, initial angular velocity is 0.0001 s^{-1} (transient motion is excluded from the simulation). Satellite is not equipped with a flywheel.

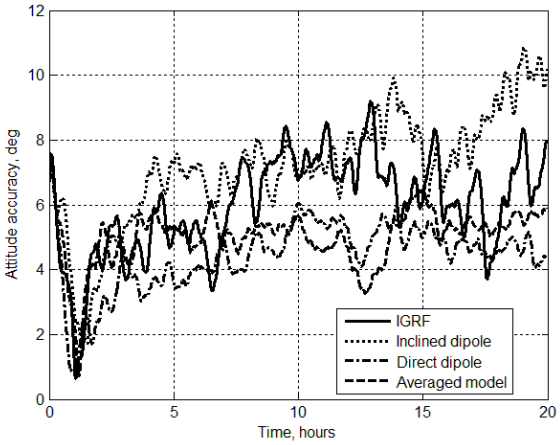

Fig. 10. Attitude accuracy in gravitational field

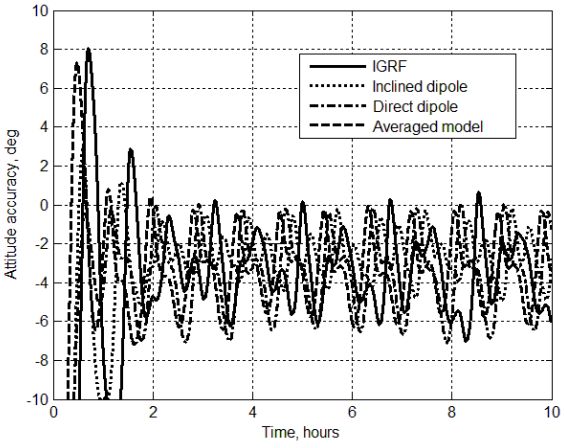

Fig. 11. Attitude accuracy with a flywheel

Attitude accuracy varies depending on the geomagnetic field model. However simplified models may be used. Fig. 11 aims at the same result for the satellite equipped with a flywheel. Magnetic control should maintain "inclined" attitude in the orbital plane. Control proposed in [49] provides rotation by 40 degrees between orbital and bound reference frames. Simplified models provide quite accurate result.

One specific case is the three-axis magnetic control discussed in [43]. Control performance is very sensitive to its parameters tuning. They are based on the geomagnetic field model. Simplified models may be used for semi-analytical control parameters selection. IGRF model should then be used in a numerical simulation for further control parameters tuning.

4. Models comparison

Recommendations for different geomagnetic field models implementation are summarized below.

IGRF/WMM – highly accurate numerical simulation; control parameters tuning on the last stages of satellite and attitude system development;

Inclined dipole – fast numerical simulation (instead or before IGRF) for transient motion and attitude accuracy;

Direct dipole model – analytical analysis in orbital and inertial frames; numerical analysis;

Averaged field – analytical analysis in inertial space, especially for transient motion.

		IGRF/ WMM	Inclined dipole	Direct dipole	Averaged
Numerical simulation	Accurate	+	∓	–	–
	Preliminary, approximate	–	+	±	∓
Motion stage	Transient	+	+	+	+
	Accuracy	+	±	±	∓
Analytical analysis	Orbital frame	–	–	+	∓
	Inertial space	–	∓	±	+

Conclusion

Four geomagnetic field models are considered: IGRF, inclined and direct dipoles, averaged field. Geomagnetic induction vector expressions are provided for different reference frames. Models are applied for analytical analysis and numerical simulation of a number of generic satellite attitude problems. Conclusions are drawn regarding models implementation for different cases according to three groups: motion nature, analysis method, reference frames used. Simplified models are shown to provide quite accurate results.

Bibliography

1. Fischell R.E. Magnetic Damping of the Angular Motions of Earth Satellites // Am. Rocket Soc. J. 1961. V. 31, № 9. pp. 1210–1217.
2. Grasshoff L.H. A Method for Controlling the Attitude of a Spin-Stabilized Satellite // ARS J. 1961. V. 31, № 5. pp. 646–649.
3. Beletsky V.V., Zonov Yu.V. Rotation and Attitude of the Third Soviet Satellite // “Artificial Earth Satellites”, USSR Academy of Scienses, 1961. № 7. pp. 32-55 (in Russian).
4. Fischell R.E. Passive Magnetic Attitude Control for Earth Satellites // Adv. Astronaut. Sci. 1963. V. 11. pp. 147–176.
5. Sarychev V.A. et al. Satellite motion in the gravitational field with hysteresis rods in the orbital plane // Cosm. Res. 1988. V. 26, № 5. p. 654–668 (in Russian).
6. Stopfkuchen K.A. A Comparison of AZUR and ESRO 1 Attitude Control System Performance // Dornier Rep. EER-A 200/69. 1969.
7. Ovchinnikov M.Y. et al. Nanosatellite REFLECTOR: Choice of Parameters of

the Attitude Control System // Cosm. Res. 2007. V. 45, № 1. pp. 60–77.
8. Ovchinnikov M. et al. Attitude Control System for the First Swedish Nanosatellite “MUNIN” // Acta Astronaut. 2000. V. 46, № 2-6. pp. 319–326.
9. Burton R., Starek J., Rock S. A New Method for Simulating the Attitude Dynamics of Passively Magnetically Stabilized Spacecraft // Adv. Astronaut. Sci. 2012. V. 143. Paper AAS 12–169.
10. Santoni F., Zelli M. Passive Magnetic Attitude Stabilization of the UNISAT-4 Microsatellite // Acta Astronaut. 2009. V. 65, № 5-6. pp. 792–803.
11. Ivanov D.S., Ovchinnikov M.Y., Penkov V.I. Laboratory study of Magnetic Properties of Hysteresis Rods for Attitude Control Systems Of Minisatellites // J. Comput. Syst. Sci. Int. 2013. V. 52, № 1. pp. 145–164.
12. Sadov Yu.A. Periodical Motion of the Satellite with Spherical Magnetic Damper in the Orbital Plane // Kosmich. Issled. 1969. V. 7, № 1. pp. 51–60 (in Russian).
13. Stickler A.C., Alfriend K.T. Elementary Magnetic Attitude Control System // J. Spacecr. Rockets. 1976. V. 13, № 5. pp. 282–287.
14. Stickler A.C. A Magnetic Control System for Attitude Acquisition // Ithaco, Inc., Rep. N 90345. 1972.
15. Guelman M. et al. Design and Testing of Magnetic Controllers for Satellite Stabilization // Acta Astronaut. 2005. V. 56, № 1-2. pp. 231–239.
16. Guo J., Bouwmeester J., Gill E. In-orbit Results of Delfi-n3Xt: Lessons Learned and Move Forward // Acta Astronaut. 2016. V. 121. pp. 39–50.
17. Candini G.P., Piergentili F., Santoni F. Miniaturized attitude Control System for Nanosatellites // Acta Astronaut. 2012. V. 81, № 1. pp. 325–334.
18. Avanzini G., Giulietti F. Magnetic Detumbling of a Rigid Spacecraft // J. Guid. Control. Dyn. 2012. V. 35, № 4. pp. 1326–1334.
19. Ovchinnikov M.Y. et al. Investigation of the Effectiveness of an Algorithm of Active Magnetic Damping // Cosm. Res. 2012. V. 50, № 2. pp. 170–176.
20. Psiaki M.L. Nanosatellite Attitude Stabilization Using Passive Aerodynamics and Active Magnetic Torquing // J. Guid. Control. Dyn. 2004. V. 27, № 3. pp. 347–355.
21. Renard M.L. Command Laws for Magnetic Attitude Control of Spin-Stabilized Earth Satellites // J. Spacecr. Rockets. 1967. V. 4, № 2. pp. 156–163.
22. Shigehara M. Geomagnetic Attitude Control of an Axisymmetric Spinning Satellite // J. Spacecr. Rockets. 1972. V. 9, № 6. pp. 391–398.
23. Artuhin Yu.P., Kargu L.I., Simaev V.L. Spin stabilized satellites control systems. Moscow: Nauka, 1979. 295 p (in Russian).
24. Hur P.S., Melton R.G., Spencer D.B. Meeting Science Requirements for Attitude Determination and Control in a Low-power, Spinning satellite // J. Aerosp. Eng. Sci. Appl. 2008. V. 1, № 1. pp. 25–33.
25. Slavinskis A. et al. High Spin Rate Magnetic Controller for Nanosatellites // Acta Astronaut. 2014. V. 95. pp. 218–226.
26. Avanzini G., de Angelis E.L., Giulietti F. Spin-axis Pointing of a Magnetically

Actuated Spacecraft // Acta Astronaut. 2014. V. 94, № 1. pp. 493–501.
27. Wheeler P.C. Spinning Spacecraft Attitude Control via the Environmental Magnetic Field // J. Spacecr. Rockets. 1967. V. 4, № 12. pp. 1631–1637.
28. Ergin E.I., Wheeler P.C. Magnetic Attitude Control of a Spinning Satellite // AIAA First Annual Meeting. 1964. AIAA Paper 64–235.
29. Sorensen J.A. A Magnetic Attitude Control System for an Axisymmetric Spinning Spacecraft // J. Spacecr. Rockets. 1971. V. 8, № 5. pp. 441–448.
30. Junkins J.L., Carrington C.K., Williams C.E. Time-Optimal Magnetic Attitude Maneuvers // J. Guid. Control. Dyn. 1981. Vo 4, № 4. pp. 363–368.
31. Sekhavat P. et al. Closed-Loop Time-Optimal Attitude Maneuvering of Magnetically Actuated Spacecraft // J. Astronaut. Sci. 2013. V. 58, № 1. pp. 81–97.
32. Biggs J.D., Horri N. Optimal Geometric Motion Planning for a Spin-Stabilized Spacecraft // Syst. Control Lett. 2012. V. 61, № 4. pp. 609–616.
33. Sarychev V.A. Problems of the Artificial Earth Satellites Attitude // Summary in Technology and Science. Series: Space Science. V.11 Moscow: VINITI, 1978. 221 p (in Russian).
34. Likins P.W. Attitude Stability Criteria for Dual Spin Spacecraft // J. Spacecr. Rockets. 1967. V. 4, № 12. pp. 1638–1643.
35. Sarychev V.A., Sazonov V.V. Nutational Dampers of Spin-Stabilized Satellites // Celest. Mech. Dyn. Astron. 1977. V. 15, № 2. pp. 225–242 (in Russian).
36. Landon V.D., Stewart B. Nutational Stability of an Axisymmetric Body Containing a Rotor // J. Spacecr. Rockets. 1964. V. 1, № 6. pp. 682–684.
37. Sandfry R.A., Hall C.D. Steady Spins and Spinup Dynamics of Axisymmetric Dual-Spin Satellites with Dampers // J. Spacecr. Rockets. 2004. V. 41, № 6. pp. 948–955.
38. Wang P., Shtessel Y., Wang Y. -q. Satellite Attitude Control Using Only Magnetorquers // Proceedings of the Thirtieth Southeastern Symposium on System Theory. Morgantown, West Virginia, 1998. pp. 500–504.
39. Psiaki M.L. Magnetic Torquer Attitude Control via Asymptotic Periodic Linear Quadratic Regulation // J. Guid. Control. Dyn. 2001. V. 24, № 2. pp. 386–394.
40. Jafarboland M. et al. Controlling the Attitude of Linear Time-Varying Model LEO Satellite Using Only Electromagnetic Actuation // IEEE Aerospace Conference Proceedings. Big Sky, Montana, 2002. pp. 2221–2229.
41. Guelman M. et al. The Gurwin-Techsat Microsatellite: Six Years Successful Operation in Space // 4S Symposium: Small Satellites, Systems and Services. La Rochelle. V. 571. p. 62.
42. Celani F. Robust Three-Axis Attitude Stabilization for Inertial Pointing Spacecraft Using Magnetorquers // Acta Astronaut. 2015. V. 107. pp. 87–96.
43. Ovchinnikov M.Y., Roldugin D.S., Penkov V.I. Three-axis Active Magnetic Attitude Control Asymptotical Study // Acta Astronaut. 2015. V. 110. pp. 279–286.
44. IGRF: http://www.ngdc.noaa.gov/IAGA/vmod/igrf.html WMM:

https://www.ngdc.noaa.gov/geomag/WMM/wmm_ddownload.shtml.
45. Antipov K.A., Tikhonov A.A. Multipole Models of the Geomagnetic Field: Construction of the Nth Approximation // Geomagn. Aeron. 2013. V. 53, № 2. pp. 257–267.
46. Zajac E.E. Some simple solutions relating to magnetic attitude control of satellites // 4th US National Congress on Applied Mechanics. Berkeley: Pergamon Press, 1962. pp. 449–456.
47. Beletsky V.V. Motion of an Artificial Satellite about its Center of Mass. Jerusalem: Israel Program for Scientific Translation, 1966.
48. Malkin I.G. Some problems in the theory of nonlinear oscillations. Oak Ridge: U.S. Atomic Energy Commission, Technical Information Service, 1959. 589 p.
49. Ovchinnikov M.Y., Roldugin D.S. Dual-spin satellite motion in magnetic and gravitational fields // Keldysh Institute Preprints. 2015. № 22. 20 p.